Interaction Between Alkyl Radicals and Single Wall Carbon Nanotubes

Pablo A. Denis

The addition of primary, secondary, and tertiary alkyl radicals to single wall carbon nanotubes (SWCNTs) was studied by means of dispersion corrected density functional theory. The PBE, B97-D, M06-L, and M06-2X functionals were used. Consideration of Van der Waals interactions is essential to obtain accurate addition energies. In effect, the enthalpy changes at 298 K, for the addition of methyl, ethyl, isopropyl, and *tert*-butyl radicals onto a (5,5) SWCNT are: −25.7, −25.1, −22.4, and −16.6 kcal/mol, at the M06-2X level, respectively, whereas at PBE/6-31G* level they are significantly lower: −25.0, −19.0, −16.7, and −5.0 kcal/mol respectively. Although the binding energies are small, the attached alkyl radicals are expected to be stable because of the large desorption barriers. The importance of nonbonded interactions was more noticeable as we moved from primary to tertiary alkyl radicals. Indeed, for the *tert*-butyl radical, physisorption onto the (11,0) SWCNT is preferred rather than chemisorption. The bond dissociation energies determined for alkyl radicals and SWCNT follow the trend suggested by the consideration of radical stabilization energies. However, they are in disagreement with some degrees of functionalization observed in recent experiments. This discrepancy would stem from the fact that for some HiPco nanotubes, nonbonded interactions with alkyl radicals are stronger than covalent bonds. © 2012 Wiley Periodicals, Inc.

DOI: 10.1002/jcc.22981

Introduction

The alkylation of single wall carbon nanotubes (SWCNTs) was developed in 1999 by Boul et al.[1] Two procedures were described to attain the synthesis of alkylated SWCNT. In the first one, fluorinated SWCNTs reacted with alkyl lithium precursors, whereas the second approach used alkyl magnesium bromides in a Grignard synthesis. The UV-vis spectroscopy unambiguously confirmed the modification of the sp^2 structure of the nanotubes by different alkyl groups. Some years later, quantitative measure of the degree of functionalization was obtained by Saini et al.[2] This analysis revealed that SWCNTs produced by the HiPco process presented a higher degree of alkylation as compared with that of laser-oven produced SWCNTs. The chemical modification was reversible if the alkylated SWCNTs were heated in Ar at 500 °C. When the HiPco SWCNTs were methylated, the carbon/alkyl group ratio was 6.6, whereas those of *n*-butyl and *n*-hexyl were 9.4 and 10.0, respectively. For the laser-oven-grown tubes, the carbon/alkyl group ratios were 6.0, 14.7, and 18.0 for methyl, *n*-butyl, and *n*-hexyl radicals, respectively. The higher degree of functionalization of HiPco SWCNTs can be explained by considering the diameter distribution of both types of nanotubes. Indeed, the diameters of laser-oven-grown SWCNTs are larger. The same year, Ying et al.[3] attached alkyl groups onto HiPco SWCNTs by the decomposition of benzoyl peroxides in the presence of alkyl iodides. TGA analysis indicated that the degree of functionalization was as high as one group per five carbons of the nanotube. Although the radical stabilization energy of $—(CH_2)_3CH_3$ is smaller than that of $—CH(CH_3)CH_2CH_3$, the amount of functionalization attained with the former was smaller. Indeed, the carbon/alkyl group ratios were 6.30 and 5.46 for $—(CH_2)_3CH_3$ and $—CH(CH_3)CH_2CH_3$, respectively. For alkyl radicals as large as $(CH_2)_{17}CH_3$, they reported a carbon/alkyl group ratio as low as 31.29. Finally, using DMSO as a source of methyl radicals, they introduced one methyl radical per 6.83 carbon atoms. Thus, again the addition of alkyl radicals as reported by Ying et al.[3] does not follow the trend expected by the consideration of the alkyl radical stabilization energies. A different route to obtain alkylated SWCNTs was proposed by Liang et al.[4] The reductive alkylation of SWCNT was achieved using lithium and alkyl halides in liquid ammonia. Finally, Georgakilas et al.[5] used aluminosilicate minerals to derivatize SWCNTs. Alkylated SWCNTs–clay composites were prepared by means of hydrothermal treatments.

The experimental evidence presented above clearly shows that SWCNTs can be alkylated yielding stable covalently functionalized SWCNTs that must be heated up to 500 °C to reverse the process. Although methyl, ethyl-like (*n*-butyl), and isopropyl-like radicals have been attached, it remains an open question if *tert*-butyl radicals can be attached to SWCNTs and why the degree of functionalization obtained in Ref. [3] does not follow the order expected by considering alkyl radical stabilization energies, that is, (primary, secondary, etc., radicals). Although a reduction of the SWCNT-R binding energies is expected because of the radical stabilization energies, it must be considered that

P. A. Denis
Computational Nanotechnology, DETEMA, Facultad de Química, UDELAR, CC 1157, 11800 Montevideo, Uruguay
E-mail: pablod@fq.edu.uy

Table 1. Electronic binding energies (kcal/mol) determined at different levels for the addition of alkyl radicals to a (5,5) SWCNT.

	PBE/DZP	PBE/6-31G*	M06-L/6-31G*	M06-L/6-31G*	M06-2X/6-31G*	B97-D/6-31G*
	∞	∞	∞	Cluster	Cluster	Cluster
CH_3	26.1(100%)	28.8(100%)	26.0(100%)	26.9(100%)	29.5(100%)	29.3(100%)
CH_2CH_3	20.2(77%)	22.3(77%)	23.5(90%)	24.2(90%)	28.4(96%)	28.6(98%)
CH_3CHCH_3	18.2(70%)	19.5(68%)	20.0(77%)	19.8(74%)	25.2(85%)	26.3(90%)
$C(CH_3)_3$	7.1(27.0)	7.3(25%)	13.7(53%)	12.4(46%)	18.9(64%)	20.8(71%)

as the number of CH_3 groups is increased when going from methyl to *tert*-butyl, CH–π interactions between the alkyl groups and the SWCNTs become more important. First principle calculations can be used to unravel the physical and chemical properties of carbon-based nanomaterials.[6–24] Herein, we investigate the addition of methyl, ethyl, isopropyl, and *tert*-butyl radicals to SWCNTs using dispersion corrected density functional theory (DFT). These calculations are intended to clarify which alkyl groups can be added to SWCNTs and what is the role of dispersion interactions during the reaction path. The addition of the $—(CH_2)_3CH_3$ and $—CH(CH_3)CH_2CH_3$ radicals was investigated to explain why the latter was more effective to functionalize SWCNTs. Finally, linear alkyl radicals as long as $(CH_2)_4CH_3$ were studied, to understand the variation of the binding energies with respect to chain length.

Methods

Density functional theory calculations were performed by means of Gaussian[25] and SIESTA.[26,27] In the case of the Gaussian calculations, the M06-2X,[28] M06-L,[28] PBE,[29] and B97-D[30] functionals were our choice. The M06-2X method is more accurate than the PBE and M06-L ones. However, periodic calculations with functionals that include exact HF exchange become complex. For this reason, at the M06-2X level, we used cluster models to investigate the addition of alkyl radicals. The $C_{80}H_{20}$ model was constructed to mimic the infinite (5,5) tube. As the metallic properties of this nanotube cannot be reproduced by a finite model, smaller reactivity is expected as compared with that corresponding to the infinite model.[31] We also note that hydrogen terminated zigzag nanotube clusters have open shell ground state.[31,32] However, to circumvent that problem, we carried out cluster model calculations using the M06-L functional. These results were compared with those obtained using infinite models, the same basis set and the M06-L functional. The outcome of this comparison was called the 'cluster effect' and was used to correct the M06-2X results. The 6-31G* basis set[33] was selected for all the Gaussian-based calculations. In the case of the PBE and M06-L periodic calculations, we included four unit cells of a (5,5) SWCNT, whereas for the (n,0) n = 8, 9, 10, 11, and 12 three unit cells were used. The largest periodic calculations involved 157 atoms and 2238 basis functions. The ultrafine grid was used for the M06-2X, M06-L, and B97-D calculations. The periodic PBE calculations conducted by means of Gaussian 2009 were intended to test the results obtained with SIESTA. These results are expected to be more accurate than those determined with SIESTA because they do not rely in the use of pseudopotentials and use basis sets of better quality like the 6-31G* one.

The calculations undertaken with SIESTA are similar to the ones that we applied to successfully study the covalent chemistry of nanotubes.[34–39] We did PBE periodic calculations in conjunction with the double-zeta basis set with polarization functions and fixed the orbital confining cutoff to 0.01 Ry. The split norm used was 0.15. The DFT implementation in SIESTA can be prone to significant basis set superposition error (BSSE), even with relatively low degree of radial confinement.[10] To avoid this problem, we used the counterpoise correction suggested by Boys and Bernardi.[40] In all cases, we used relaxed structures to estimate the BSSE-corrected binding energies, and we took monomer deformation energies into account. The interaction between ionic cores and valence electrons was described by the Troullier–Martins norm conserving pseudopotentials.[41] We have checked the convergence of the Mesh cutoff; using a value of 200 Ry, we obtained converged binding energies (within 0.02 eV). For the (5,5) SWCNTs, we selected four unit cells to model the metallic tube and two for the semiconducting one. The lattice parameter along the c direction was fixed to 9.84 Å for the (5,5) and the a and b directions were fixed to 20 Å, a value large enough to prevent the interaction between adjacent images. Bearing in mind, the symmetry of the SWCNTs, we used a Monkhorst–Pack sampling of $1 \times 1 \times 300$.

Results and Discussion

The electronic reaction energies determined for the addition of the methyl, ethyl, isopropyl, and *tert*-butyl radicals to SWCNTs are presented in Table 1 and the SWCNT-alkyl bond distances in Table 2. The structures of the functionalized (5,5) SWCNTs are shown in Figure 1. Periodic calculations at the PBE/6-31G* and PBE/DZP levels gave similar results. The reaction energy for ethylation is a 77% of the value determined for CH_3, for isopropyl it decreases to 68%, whereas for *tert*-butyl it is only a 25%. The whole picture notably changes when the M06-L/6-31G* method is considered. For CH_2CH_3, the binding energy is increased by a 13% that of isopropyl by a 7% and *tert*-butyl shows the most dramatic change by 28%. The differences observed between the

Table 2. SWCNT-R bond distances (Å) determined at various levels, R= methyl, ethyl, isopropyl, and *tert*-butyl.

	PBE/ DZP	PBE/ 6-31G*	M06-L/ 6-31G*	M06-L/ 6-31G*	M06-2X/ 6-31G*	B97-D/ 6-31G*
	∞	∞	∞	Cluster	Cluster	Cluster
CH_3	1.564	1.564	1.550	1.550	1.553	1.565
CH_2CH_3	1.579	1.579	1.564	1.562	1.563	1.576
CH_3CHCH_3	1.605	1.604	1.587	1.587	1.584	1.600
$C(CH_3)_3$	1.640	1.645	1.624	1.623	1.617	1.639

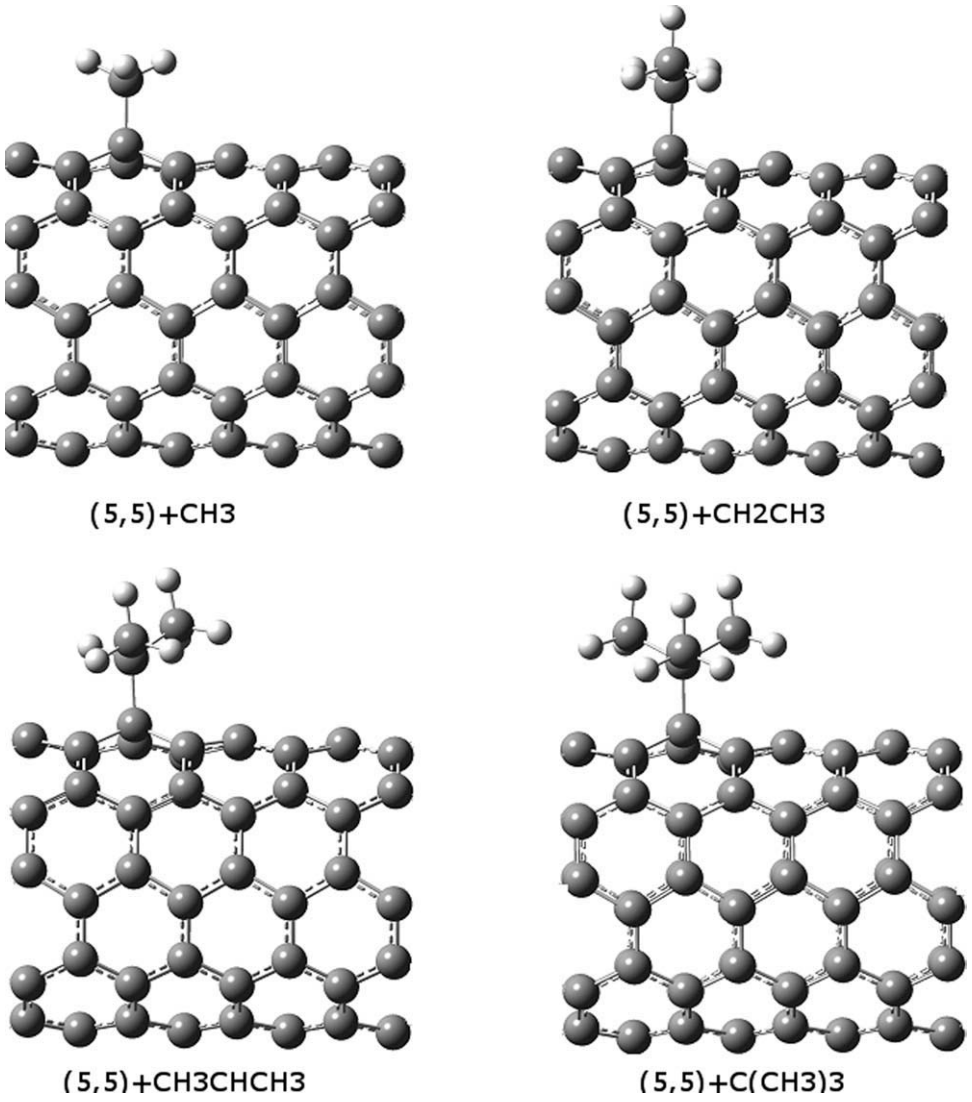

Figure 1. Optimized unit cells for the addition of alkyl radicals to a (5,5) SWCNT.

PBE and M06-L results can be attributed to the fact that PBE does not work well for CH–π interactions. These types of forces are increased as the number of CH_3 groups becomes larger. Although the M06-L method is a good choice for periodic systems, M06-2X works better for bonded and nonbonded interactions.[28] At the M06-2X level and using a $C_{80}H_{20}$ cluster, we found that the binding energy of *tert*-butyl is a 68% of the value determined for the methyl radical, almost two and a half times the value determined at the PBE level. For ethyl and isopropyl radicals, the values are also increased, climbing up to 96 and 85%, respectively. The differences between M06-2X and PBE can be appreciated with more details in Figure 2, where we plot the reaction energies determined at the PBE/6-31G* and M06-2X/6-31G* levels.

It is possible that the huge changes observed with M06-2X were due to the used of cluster models. For this reason, we performed cluster model calculations at the M06-L/6-31G* level of theory. Although there are small numerical differences between the absolute values of the electronic binding energies determined using finite and infinite models, the % of the binding energies corresponding to ethyl, isopropyl, and *tert*-butyl are essentially the same. Another problem that may affect the M06-2X results is that this method does not capture enough long range correlation. Taking this observation into account, we carried out calculations with Grimme's dispersion corrected B97-D functional.[29] The latter results are in excellent agreement with those obtained with the M06-2X functional. In effect, for the *tert*-butyl radical, the binding energy is a 71% of the value computed for CH_3, whereas M06-2X suggested a smaller value, 64%. This difference may be attributed to the fact that M06-2X does not have the correct asymptotic behavior and it underestimates noncovalent interactions in positions far from the equilibrium,[42,43] even though it has been reported that M06-L is too attractive at distances shorter than equilibrium.[44]

The comparisons presented in the previous paragraph led us to two important findings. In the first place, the strong increase of the binding energies observed at the M06-2X and B97-D levels is not an artifact of the cluster models used. Last but not least, the electronic binding energies determined at the M06-2X level and using cluster models are expected to be within 1 kcal/mol to the value that we would compute if periodic conditions were to be used. Therefore, we can estimate the electronic binding energies of methyl, ethyl, isopropyl, and *tert*-butyl radicals to a

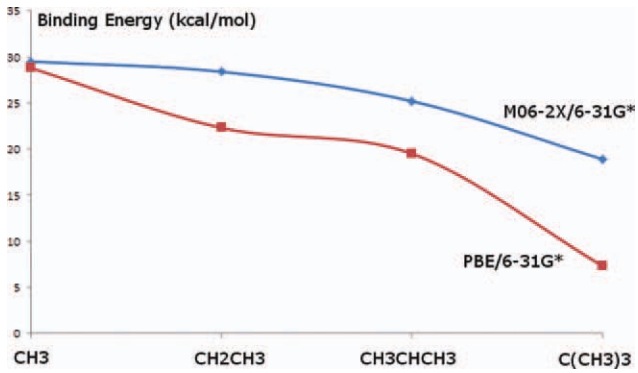

Figure 2. Binding energy of alkyl radicals and a (5,5) SWCNT, calculated at the M06-2X/6-31G* and PBE/6-31G* levels of theory.

(5,5) SWCNT as 30, 28, 25, and 19 kcal/mol, respectively. In previous works,[10,34] we have shown that the change from electronic reaction energies to reaction free energies (ΔG°_{298}) is almost independent of the carbon structure studied. For example, in the case of the 1,3 dipolar cycloaddition of azomethine ylides to ethene, pyrene, and a $C_{48}H_{18}$ graphene flake, we found that the difference ΔE–ΔG is 0.84, 0.82, and 0.82 kcal/mol, respectively. Thus, we concluded that for a larger nanostructure, it would be similar. Taking this finding into account, we estimated the enthalpy and free energies changes for the addition of alkyl radicals onto a (5,5) SWCNT using the thermodynamic data determined for the $C_{80}H_{20}$ cluster. Using this procedure, we found that the enthalpy changes at 298 K are −25.7, −25.1, −22.4, and −16.6 kcal/mol for the addition of methyl, ethyl, isopropyl, and *tert*-butyl radicals, respectively. At the same temperature and 1 atm, the ΔG°_{298} are −15.1, −12.9, −9.1, and −2.8 kcal/mol, for methyl, ethyl, isopropyl, and *tert*-butyl radicals, respectively. Thus, at 298 K the addition of the four alkyl radicals studied onto the (5,5) SWCNT is spontaneous, even though most of them are expected to become positive as the diameter is increased.

The effect of diameter on the addition of alky radicals was investigated considering the (*n*,0) $n = 8$, 9, 10, 11, and 12 SWCNTs. The results are presented in Table 3. As curvature decreases, we observe an important diminution of the electronic binding energies, even though for the (9,0) and (12,0) SWCNTs their semimetallic character compensates the increase of diameter. When going from the (8,0) SWCNT to the (11,0) one the electronic binding energies are reduced by 6.6 and 6.2 kcal/mol, at the M06-L/6-31G* level, for the CH_3 and $C(CH_3)_3$ radicals, respectively. Regarding the comparative performance of M06-L and PBE, we can appreciate that the results are in line with those obtained for the (5,5) SWCNT: PBE always suggests lower binding energies. For the (11,0) SWCNT, the electronic binding energy of the *tert*-butyl radical is only 5.4 kcal/mol. Considering that this radical is quite bulky, it may be possible that physisorption is preferred over chemisorption. At the M06-L/6-31G* level, we found that the electronic adsorption energy of $C(CH_3)_3$ onto the (11,0) SWCNT is 7.4 kcal/mol. Thus, the Van der Waals interaction energy is 2 kcal/mol larger than that computed for the covalently bonded structure. For the isopropyl radical, a similar effect is expected. However, it will occur at a slightly larger diameter because the covalent bond between the SWCNTs and CH_3CHCH_3 is stronger than that of *tert*-butyl.

Table 3. Electronic binding energies (kcal/mol) determined at different levels for the covalent addition of CH_3 and $C(CH_3)_3$ radicals to SWCNTs.

		M06-L/6-31G*		PBE/6-31G*	
	Diameter	CH_3	$C(CH_3)_3$	CH_3	$C(CH_3)_3$
(8,0)	6.3	26.4	11.6(44%)	29.7	10.0(34%)
(9,0)	7.1	26.0	11.6(45%)		
(5,5)	6.9	26.0	13.7(53%)	28.8	7.3(25%)
(10,0)	8.0	21.3	6.9(32%)		
(11,0)	8.6	19.8	5.4(27%)	22.6	2.9(13%)
(12,0)	9.4	19.9	5.6(28%)		

In the previous paragraph, we attributed the low values determined for the addition of bulkier alkyl radicals at the PBE/6-31G* level, to the fact that PBE does not accurately treats dispersion interactions. For the sake of completeness, we studied the CH_4—C_6H_6 complex. At the CCSD(T)/CBS limit, Shibasaki et al.[45] reported that the D_e of the methane–benzene cluster is 1.43 kcal/mol. For a related complex, the o-quinodimethane adducts of C_{60}, variable temperature NMR studies suggested that the lower limit for each aryl CH-fullerene π interaction is 0.95 kcal/mol,[46] in good agreement with the value determined for the CH_4—C_6H_6 complex. For the latter system, we found that the interaction energies are 0.7, 1.2, and 1.5 kcal/mol at the PBE/6-31G*, M06-L/6-31G*, and M06-2X/6-31G* levels, respectively, Thus, M06-2X is in excellent agreement with the CCSD(T)/CBS value, but PBE underestimates the CH–π interaction energies by a 50%. Although the M06-L method is closer to the M06-2X result, it is short by a 50%. Therefore, we can conclude that the trend observed for the CH_4—C_6H_6 complex follow the same as that observed for the addition of alkyl radicals to SWCNTs, PBE gives the lowest binding energies and M06-2X the largest ones. Although we have shown that PBE and M06-L underestimates CH–π interactions as compared with M06-2X, as the interaction of alkyl radicals and SWCNT has covalent and noncovalent characteristics, it is possible to argue that the large binding energies determined at the M06-2X level are due to an overestimation of the C—C binding energies at the M06-2X level. For this reason, we studied the bond dissociation energy of ethane. Using the values reported by Feller et al.[47] at the CCSD(T)/CBS level and including all the minor corrections, $D_e = 97.2$ kcal/mol, whereas it is predicted to be 109.4, 99.6, and 102.51 kcal/mol at the PBE/6-31G*, M06-L/6-31G*, and M06-2X levels, respectively. Therefore, PBE overestimates the BDE of ethane by 12.2 kcal/mol and M06-2X by 5.3 kcal/mol. This comparison supports that the root of the discrepancy for the results presented in Table 1 is the bad treatment of dispersion interactions by PBE.

The bad performance of density functionals that not include dispersion effects is known for providing an incorrect description of reaction paths. One of the most recent examples is the Diels–Alder reaction between C_{60} and cyclopentadiene. In effect, Osuna et al.[48] showed that the lack of dispersion interactions in B3LYP introduced errors as large as 16.4 and 15.4 kcal/mol for the reaction exothermicity and activation barriers, respectively. In the same vein, Catak et al.[49] demonstrated that dispersion corrected density functionals like M06-2X must be used to study the interaction between organophosphorous compounds and coke surface. As dispersion effects are very important to study the reactivity of carbon-based nanomaterials,[50–52] it is interesting to gauge their role in the reaction path. In Figure 3, we show the reaction path for the addition of the CH_3 radical to the (5,5) SWCNT, calculated at the PBE/6-31G* and M06-2X/6-31G* levels of theory, respectively and using a $C_{80}H_{20}$ cluster. The main difference between the PBE and M06-2X reaction paths is the stabilization energy of the precursor complex. For the methyl radical, PBE/631G* indicates a stabilization energy of 1.6 kcal/mol with respect to the dissociated products. However, M06-2X suggests a larger value, namely, 6.4 kcal/mol. The transition state is located 0.7 and 2.9 kcal/mol above the reactants at

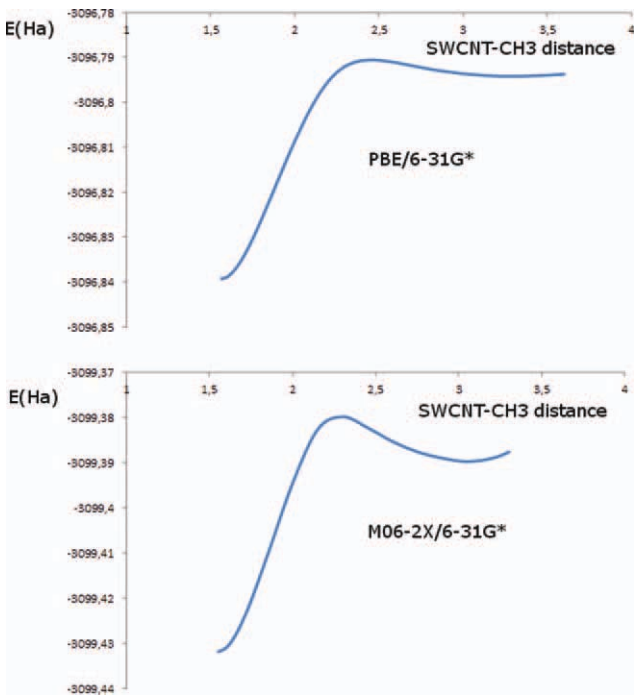

Figure 3. Reaction path determined for the addition of methyl radical to a (5,5) SWCNT.

the PBE/6-31G* and M06-2X/6-31G* levels of theory, respectively. The reaction barrier for the addition of the methyl radical notably changes when entropy is included. Indeed, $\Delta G^{\ddagger} = 11.4$ and 12.8 kcal/mol at the PBE/6-31G* and M06-2X/6-31G* levels of theory, respectively. In contrast with the low reaction barriers determined for the attachment of alkyl radicals, the desorption barriers are significantly larger and thus explain the experimentally evidence supporting the thermal stability of the attached alkyl radicals. At the M06-2X/level, the electronic desorption barrier is 32.4 kcal/mol and free energy desorption barrier is 28.0 kcal/mol. In the case of the CH_3CHCH_3 radical, we have also followed the reaction path and the whole picture is similar, the main difference between M06-2X and PBE is the stabilization of the precursor complex. The electronic desorption barrier of CH_3CHCH_3 is slightly smaller, 24 kcal/mol, mostly due to the lower binding energy of the isopropyl radical.

Finally, it is interesting to compare the effect of the alkyl chain length on the reaction energies. In Table 4, we list the reaction energies for the addition of $(CH_2)_nCH_3$ radicals, $n = 1, 2, 3, 4$. The electronic binding energies determined for these radicals are similar. Moreover, the ΔG°_{298} are within a range of 1 kcal/mol. Thus, the large carbon/alkyl group ratio (31.29) determined by Ying et al.[3] for $(CH_2)_{17}CH_3$ cannot be attributed to a thermodynamic effect but to a kinetic one, due to the size of the alkyl radical used. The last comparison that we performed with experiment is for the addition of $(CH_2)_3CH_3$ and $CH(CH_3)CH_2CH_3$ radicals. In contrast with the levels of functionalization attained with both radicals (6.30 and 5.46, respectively), we found that the electronic binding energy determined for the $CH(CH_3)CH_2CH_3$ radical is 24.0 kcal/mol, about 2 kcal/mol smaller than that computed for $(CH_2)_3CH_3$. Although the levels of functionalization reported may have some error, it may be possible that for the high end of the diameter distribution of the HiPco SWCNTs, the physisorption of the $CH(CH_3)CH_2CH_3$ radical may be stronger than the covalent bond formed by the $(CH_2)_3CH_3$ radical, as we discussed above for the addition of the *tert*-butyl radical onto the (11,0) SWCNTs.

Table 4. Binding energies (kcal/mol) determined for $-(CH_2)_nCH_3$ radicals $n = 2, 3, 4, 5$, at the M06-2X level of theory.

	ΔE_e	ΔG_{298}
CH_2CH_3	28.4	−12.9
$CH_2CH_2CH_3$	27.4	−12.0
$CH_2CH_2CH_2CH_3$	26.0	−12.0
$CH_2CH_2CH_2CH_2CH_3$	27.5	

Conclusions

We have studied the addition of primary, secondary, and tertiary alkyl radicals to SWCNTs using the PBE, B97-D, M06-L, and M06-2X functionals, respectively. The inclusion of dispersion is essential to obtain accurate reaction energies. In effect, for the addition of the *tert*-butyl radical onto the (5,5) SWCNT, PBE underestimated the binding energy by 13 kcal/mol with respect to B97-D. The importance of nonbonded interactions was more noticeable as we moved from primary to tertiary alkyl radicals. The enthalpy changes for the addition of methyl, ethyl, isopropyl, and *tert*-butyl radicals onto a (5,5) SWCNT are −25.6, −25.1, −22.4, and −16.6 kcal/mol. Although the binding energies are small, the alkyl radicals are expected to be stable because of the large desorption barriers. In the case of CH_3 and CH_3CHCH_3, they are 28.0 and 19.6 kcal/mol, respectively. The bond energies determined for alkyl radicals and SWCNT follow the trend suggested by the consideration of radical stabilization energies. However, they are in disagreement with the degrees of functionalization observed in recent experiments.[3] The source of this discrepancy maybe related to the fact that at a certain diameter the physisorption is alkyl radicals is preferred over chemisorption. The binding energies of alkyl radicals do not show noticeable changes as the chain length was increased. Thus, the low reactivity experimentally observed for long alkyl radicals can be attributed to a kinetic effect.

Acknowledgments

The author thanks PEDECIBA Quimica for financial support.

Keywords: carbon nanotubes · alkylation · free radicals · nanotechnology · organic chemistry

How to cite this article: P. A. Denis, *J. Comput. Chem.* **2012,** *33,* 1511–1516. DOI: 10.1002/jcc.22981

[1] P. J. Boul, J. Liu, E. T. Mickelson, C. B. Huffman, L. M. Ericson, I. W. Chiang, K. A Smith,. D. T. Colbert, R. H. Hauge, J. L. Margrave, R. E. Smalley, *Chem. Phys. Lett.* **1999**, *310,* 367.

[2] R. K. Saini, I. W. Chiang, H. Peng, R. E. Smalley, W. E. Billups, R. H. Hauge, J. L. Margrave, *J. Am. Chem. Soc.* **2003**, *125,* 3617.

[3] Y. Ying, R. K. Saini, F. Liang, A. K. Sadana, W. E. Billups, *Org. Lett.* **2003**, *5,* 1471.
[4] F. Liang, A. K. Sadana, J. Chattopadhyay, Z. Gu, R. H. Hauge, W. E. Billups, *Nano Lett.* **2004**, *4,* 1257.
[5] V. Georgakilas, D. Gournis, M. A. Karakassides, A. Bakandritsos, D. Petridis, *Carbon* **2004**, *42,* 865.
[6] H. Y. He, B. C. Pan, *J. Phys. Chem. C,* **2008**, *112,* 18876.
[7] P. A. Denis, F. Iribarne, *J. Phys.Chem. C* **2011**, *115,* 195.
[8] K. Suggs, D. Reuven, X. Q. Wang, *J. Phys. Chem. C* **2011**, *115,* 3313.
[9] N. Ghaderi, M. Peressi, *J. Phys. Chem. C,* **2010**, *114,* 21625.
[10] P. A. Denis, *J. Phys.Chem. C,* **2009**, *113,* 5612.
[11] P. A. Denis, *J. Phys.Chem. C,* **2011**, *115,* 13392.
[12] Y. Yu, S. Yuan, J. Xu S. Wu, *Russ. J. Phys. Chem. A,* **2011**, *85,* 1031.
[13] P. A. Denis, F. Iribarne, *J. Phys.Chem. C* **2011**, *115,* 56.
[14] P. Chandrachud, B. S. Pujari, S. Haldar, B. Sanyal, D. K. Kanhere, *J. Phys.: Condens. Matter* **2010**, *22,* 465502.
[15] P. A. Denis, R. Faccio, A. W. Mombru, *ChemPhysChem.* **2009**, *10,* 715.
[16] P. A. Denis, F. Iribarne, *F. J. Mol. Struct. Theochem.* **2009**, *907,* 93.
[17] Z. M. Ao, J. Yang, S. Li and Q. Jiang, *Chem. Phys. Lett.* **2008**, *461,* 276.
[18] Z. M. Ao, J. Yang, S. Li and Q. Jiang, *Phys. Chem. Chem. Phys.* **2009**, *11,* 1683.
[19] P. A. Denis, *Chem. Phys. Lett.* **2010**, *492,* 251.
[20] P. A. Denis, *Chem. Phys Lett.* **2011**, *508,* 95.
[21] N. Al-Aqtash, I. Vasiliev, *J. Phys.Chem. C* **2009**, *113,* 12970.
[22] J. Dai, J. Yuan, P. Giannozzi, *Appl. Phys. Lett.* **2009**, *95,* 232105.
[23] J. Dai, J. Yuan, *J. Phys.: Condens. Matter* **2010**, *22,* 225501.
[24] S. J. Gong, W. Sheng, J. H. Chu, *J. Phys.: Condens. Matter* **2010**, *22,* 245502.
[25] Gaussian 09, Revision A.1, M. J. Frisch, G. W. Trucks, H. B. Schlegel, G. E. Scuseria, M. A. Robb, J. R. Cheeseman, G. Scalmani, V. Barone, B. Mennucci, G. A. Petersson, H. Nakatsuji, M. Caricato, X. Li, H. P. Hratchian, A. F. Izmaylov, J. Bloino, G. Zheng, J. L. Sonnenberg, M. Hada, M. Ehara, K. Toyota, R. Fukuda, J. Hasegawa, M. Ishida, T. Nakajima, Y. Honda, O. Kitao, H. Nakai, T. Vreven, J. A. Montgomery, Jr., J. E. Peralta, F. Ogliaro, M. Bearpark, J. J. Heyd, E. Brothers, K. N. Kudin, V. N. Staroverov, R. Kobayashi, J. Normand, K. Raghavachari, A. Rendell, J. C. Burant, S. S. Iyengar, J. Tomasi, M. Cossi, N. Rega, J. M. Millam, M. Klene, J. E. Knox, J. B. Cross, V. Bakken, C. Adamo, J. Jaramillo, R. Gomperts, R. E. Stratmann, O. Yazyev, A. J. Austin, R. Cammi, C. Pomelli, J. W. Ochterski, R. L. Martin, K. Morokuma, V. G. Zakrzewski, G. A. Voth, P. Salvador, J. J. Dannenberg, S. Dapprich, A. D. Daniels, Ö. Farkas, J. B. Foresman, J. V. Ortiz, J. Cioslowski, and D. J. Fox, Gaussian 09, Revision A.1, Gaussian, Wallingford CT, **2009**;
[26] J. M. Soler, E. Artacho, J. D. Gale, A. Garcia, J. Junquera, P. Ordejon, D. Sanchez-Portal, *J. Phys.: Condens. Matter* **2002**, *14,* 2745.
[27] P. Ordejon, E. Artacho, J.M. Soler, *Phys. Rev. B* **1996**, *53,* R10441.
[28] Y. Zhao, D. G. Truhlar, *J. Chem. Phys.* **2006**, *125,* 194101.
[29] J. P. Perdew, K. Burke, M. Ernzerhof, *Phys. Rev. Lett,* **1996**, *77,* 3865.
[30] S. Grimme, *J. Comp. Chem.,* **2006**, *27,* 1787.
[31] P. A. Denis, F. Iribarne, *J. Comput. Chem.* **2011**, *32,* 2397.
[32] J. Du, Y. Chen, G.Q. Lu, S.C. Smith, *Appl. Phys. Lett.* **2008**, *93,* 073101.
[33] R. Ditchfeld, W. J. Hehre, J. A. Pople, *J. Chem. Phys.* **1971**, *54,* 724.
[34] P. A. Denis, F. Iribarne, *Int. J. Quantum Chem.* **2010**, *110,* 1764.
[35] P. A. Denis, R. Faccio, *Chem. Phys. Lett.,* **2008**, *460,* 486.
[36] P. A. Denis, *Int. J. Quant. Chem.,* **2009**, *109,* 772.
[37] P. A. Denis, J. S. Gancheff, *J. Mater. Sci.* **2010**, *45,* 1039.
[38] P. A. Denis, F. Iribarne, R. Faccio, *J. Chem. Phys.,* **2009**, *130,* 194704.
[39] P. A. Denis, *J. Phys. Chem. C* **2011**, *115,* 20282.
[40] F. S. Boys, F. Bernardi, *Mol. Phys.* **1970**, *19,* 553.
[41] N. Troullier, J. L. Martins, *Phys. Rev. B* **1991**, *43,* 1993.
[42] E. G. Hohenstein, S. T. Chill, C. D. Sherrill, *J. Chem. Theory Comput.* **2008**, *4,* 1996.
[43] K. E. Riley, M. Pitonak, P. Jurecka P. Hobza, *Chem. Rev.* **2010**, *110,* 5023.
[44] D. Benitez, E. Tkatchouk, I. Yoon, J. F. Stoddart W. A. Goddard, *J. Am. Chem. Soc.* **2008**, *130,* 14928.
[45] K. Shibasaki, A. Fuji, N. Mikami S. Tsuzuki, *J. Phys. Chem. A* **2006**, *110,* 4397.
[46] R. P. Kopreski, J. B. Briggs, W. Lin, M. Jazdzyk, G. P. Miller, *J. Org. Chem.* **2012**, *77,* 1308.
[47] D. Feller, K. A. Peterson, D. A. Dixon, *J. Chem. Phys.* **2008**, *129,* 204105.
[48] S. Osuna, M. Swart, M. Sola, *J. Phys. Chem. A* **2011**, *115,* 3491.
[49] S. Catak, K. Hemelsoet, L. Hermosilla, M. Waroquier, V. Van Speybroek, *Chem. Eur. J.* **2011**, *17,* 12027.
[50] S. Krishnan, R. Vadapoo, K. E. Riley, J. P. Velev, *Phys. Rev. B* **2011**, *84,* 165408.
[51] K. Suggs, V. Person, X. Q. Wang, *Nanoscale* **2011**, *3,* 2465.
[52] R. N. Gunasinghe, C. B. Kah, K. D. Quarles, X. Q. Wang, *Appl. Phys. Lett.* **2011**, *98,* 261906.

Received: 4 January 2012
Revised: 21 February 2012
Accepted: 10 March 2012
Published online on 23 April 2012